Bull. Chem. Soc. Jpn., 72, 1239—1246 (1999)

X-Ray Absorption Fine Structure (XAFS) Studies on Cobalt(II) Bromo Complexes in Acetic Acid Solutions

Toshio Akai,* Masami Okuda, and Masaharu Nomura†

Yokohama Research Center, Mitsubishi Chemical Corporation, 1000 Kamoshida-cho, Aoba-ku, Yokohama 227-8502

†Institute of Materials Structure Science, High Energy Accelerator Research Organization, Oho 1-1, Tsukuba 305-0801

(Received December 21, 1998)

X-Ray absorption fine structure (XAFS) studies were performed for cobalt(II) bromo complexes prepared for the ratio Br/Co from 0.0 to 4.0 and for their oxidized complexes with ozone in acetic acid solvent. The multivariate curve resolution method indicates the existence of two kinds of chemical species both before and after the oxidation. Before oxidation, the two species are cobalt(II) acetate and tetrahedral cobalt(II) complex coordinated by Br. The oxidized sample with ozone consists of cobalt(II) acetate and trinuclear cobalt(III) complex; however, cobalt(III) complexes including Br are not detected. The rate of the change from the cobalt(II) complex coordinated by Br to the trinuclear cobalt(III) complex is lower than that from cobalt(II) acetate complex. This indicates that the tetrahedral cobalt(II) complex coordinated by Br is more difficult to be oxidized than the octahedral cobalt(II) acetate complex.

The bromo complex of cobalt(II) acetate plays an important role in a variety of liquid phase oxidation reactions. Its oxidized form can be used as a homogeneous catalyst for auto-oxidations of organic materials. These include the conversion of *p*-xylene to terephthalic acid, the oxidation of butane to acetic acid, and the oxidation of cyclohexane to cyclohexanone, and even to adipic acid.[1] These autoxidations are commonly observed in acetic acid solution. The selectivity or efficiency of a catalyst depends on the ratio of cobalt to bromine, so it is important to study the cobalt(II) bromo complexes and their oxidized complexes in acetic acid solutions in order to improve catalytic performance and develop a new catalysis. In particular, the structural information of these complexes is quite useful when we consider the roles of the complexes in such autoxidations, because these are not clear yet.

There have been many studies on the cobalt(II) bromo complexes in acetic acid solutions with UV-visible spectra.[2] UV-visible spectroscopy is an easy and useful method to investigate the electronic state of the cobalt complexes; the color of the solution changes from pink to blue as the Br content increases. It is difficult, however, to extract structural information from the spectra although the pink and blue colors have empirically been related to octahedral and tetrahedral Co complexes, respectively. Molecular orbital calculations are necessary to obtain the structural information from UV-visible spectra. The calculation of the excitation spectra, however, takes a long time, and the accuracy is not so good for complicated systems as for the Co complexes.

X-Ray absorption fine structure (XAFS) is a powerful tool to obtain structural information around an X-ray absorbing atom even in solution. Several XAFS studies of cobalt(II) bromo complexes have been carried out.[3,4] There has been no report on cobalt(II) bromo complexes in acetic acid solutions, however. Blake et al. studied some kinds of oxidized cobalt(II) acetates with the use of XAFS, but the acetates did not contain Br.[5] They reported that trinuclear oxo-centered Co complexes were produced by the oxidation of cobalt(II) acetate.

We carried out XAFS studies of some cobalt(II) bromo complexes prepared in different atomic ratios of Br to Co (Br/Co) and related complexes oxidized with ozone in acetic acid. In this paper, we separate out each of the spectra from the observed X-ray absorption near edge structure (XANES) spectra by the use of the multivariate curve resolution method and analyze the results with the XANES fingerprint method. The result of this technique is also applied to the extended X-ray absorption fine structure (EXAFS) analyses. The main purpose of this study is to obtain structural information on the cobalt(II) bromo complexes and their oxidized complexes in acetic acid solutions from XAFS analyses.

Experimental

The inorganic materials used as reagents were analytical grade $Co(CH_3COO)_2 \cdot 4H_2O$ and NaBr. They were dissolved in reagent-grade glacial acetic acid without further purification. The oxidation was carried out for two hours with ozone, the concentration of which was 197 ppm at 10 $cm^3 min^{-1}$ flow. Six different samples with different atomic ratios of Br/Co (0.0, 0.25, 0.5, 1.0, 2.0, 4.0), in which the concentration of Co was fixed to 0.15 mol%, were prepared. Each of them were oxidized with ozone for two hours. The oxidation condition used by Blake et al. was considered;[5] however, the oxidation condition of this study was finally determined by use of the results of UV-visible spectra. This was in order to emphasize the difference among the samples after oxidation. All solution samples were sealed in poly(tetrafluoroethylene) cells with polyimide windows. It was confirmed that there was no change in the sam-

ples before and after the XAFS measurement. We also measured the X-ray absorption spectrum of pure acetic acid as a background spectrum to subtract the pre-edge spectrum.

Co K-edge XAFS spectra were measured in the fluorescence mode at the BL12C of the Photon Factory at the High Energy Accelerator Research Organization (KEK),[6] running at 2.5 GeV, with a beam current of 200 to 300 mA. X-Rays were monochromatized by a Si(111) double-crystal monochromator, and intensity was measured by a 17 cm long ionization chamber filled with nitrogen. The fluorescent X-rays were detected by the detector developed by Lytle et al.,[7] which was filled with pure argon gas. An iron filter ($\mu t = 3$) was used in order to minimize the scattering X-rays.

We also measured the XAFS spectra of cobalt(II) acetate tetrahydrate ($Co(CH_3COO)_2 \cdot 4H_2O$) and tris(acetylacetonato)cobalt(III) ($[Co(acac)_3]$) as reference samples in powder. These solid samples were mixed with cellulose powders and pressed into disks for the XAFS measurement. They were measured in transmission mode at room temperature. The XAFS spectrum of Fe foil was measured for the energy calibration at the beginning and the end of the XAFS measurements, and we confirmed that there was no energy shift during the measurements.

Method of Analysis

1. EXAFS. The pre-edge background of the Co K-edge XAFS spectrum was subtracted from the raw XAFS spectrum by use of the measured background spectrum of acetic acid. The cubic spline method was used to remove the post-edge background. For edge normalization, extraction of the EXAFS signal $\chi(k)$, and the Fourier transform of $\chi(k)$, where k is the photoelectron wave vector, we used the conventional technique.[8] The Fourier transforms were performed in the k range of 3.15 to 11.35 $Å^{-1}$ for before oxidation, and of 3.32 to 11.52 $Å^{-1}$ for after oxidation. The curve fitting calculations were carried out in the R range of 1.21 to 2.12 Å for one shell, of 1.21 to 2.42 Å for two shells, and of 1.00 to 3.16 Å for three shells, where R is the distance without phase correction. The phase shift and the back-scattering amplitude were derived from the theoretical program feff5.[9] The edge shift ΔE_0 was estimated by use of the simulated spectra of some model structures with feff5, and was fixed in the curve fitting calculations. The Debye–Waller factor in the calculations was treated as a variable parameter. The amplitude reduction factor in feff5, S_0^2, was estimated from the spectrum of $Co(CH_3COO)_2 \cdot 4H_2O$. We estimated that the range of error of the inter-atomic distance was plus or minus 0.02 Å and the range of error of the coordination number was plus or minus 10%.

2. XANES. The solutions prepared in this work contain two or more different kinds of complexes whose concentrations follow the chemical equilibrium condition, so it is important to extract a spectrum and a concentration of each component from the observed complicated XANES spectra before analyzing them. Multivariate curve resolution methods are quite useful for this purpose. The application of the multivariate curve resolution method called Target Factor Analysis (TFA) to XANES spectra has been reported in some studies.[10,11] However, the measured spectra which are expected to be included in data set have to be available beforehand to apply the TFA method.[12] It is sometimes difficult to get these spectra. We therefore used the multivariate curve resolution method called Alternating Least Squares (ALS) calculation in which these spectra are not necessary.[13,14]

Prior to this analysis, pre-edge subtraction and normalization of XANES were performed by use of the same method as that for EXAFS. The spectral data were arranged in a matrix form, $\boldsymbol{D}$, with one spectrum per row. The rows correspond to the spectra, and the columns correspond to photon energy values in the spectra.

Data matrix $\boldsymbol{D}$, consisting of l (the number of spectra) rows and m (the number of the data points of the XANES spectrum) columns with $l \leqq m$, can be decomposed as follows by the method called singular value decomposition (SVD):[15]

$$\boldsymbol{D} = \sum_{i=1}^{l} s_i \boldsymbol{u}_i \boldsymbol{v}_i^{\mathrm{T}} = \boldsymbol{U}\boldsymbol{S}\boldsymbol{V}^{\mathrm{T}}. \tag{1}$$

Here $\boldsymbol{u}_i$ and $\boldsymbol{v}_i$ are orthonormal column eigenvectors, and $\boldsymbol{U}$ and $\boldsymbol{V}$ are orthonormal matrices.[15] The superscript notation, $\boldsymbol{v}_i^{\mathrm{T}}$, $\boldsymbol{V}^{\mathrm{T}}$ means the transpose of the vector $\boldsymbol{v}_i$ and the matrix $\boldsymbol{V}$, respectively. $\boldsymbol{S}$ is a diagonal matrix whose diagonal elements s_i are called singular values. They are equal to the square roots of the eigenvalues associated with the matrix $\boldsymbol{D}\boldsymbol{D}^{\mathrm{T}}$, $\boldsymbol{D}^{\mathrm{T}}\boldsymbol{D}$. Since the significant singular values are to be related to the pure chemical species, we estimated the number of the pure chemical species by evaluating the magnitude of singular values.

If $\boldsymbol{D}$ contains n pure chemical species ($n \leqq l$), $\boldsymbol{D}$ is written as

$$\boldsymbol{D} = \overline{\boldsymbol{D}} + \boldsymbol{E}, \tag{2}$$

where

$$\overline{\boldsymbol{D}} = \sum_{i=1}^{n} s_i \boldsymbol{u}_i \boldsymbol{v}_i^{\mathrm{T}}, \tag{3}$$

$$\boldsymbol{E} = \sum_{i=n+1}^{l} s_i \boldsymbol{u}_i \boldsymbol{v}_i^{\mathrm{T}}. \tag{4}$$

Here, $\overline{\boldsymbol{D}}$ is reproduced with the matrices related to the n physically meaningful singular values and $\boldsymbol{E}$ is the residual matrix which is related to error. We used the reproduced data matrix $\overline{\boldsymbol{D}}$ in the calculation of pure component spectra and concentrations because the raw data matrix $\boldsymbol{D}$ can include experimental error.

The multivariate curve resolution method called ALS was used to extract pure component spectra.[13,14] A measured XANES spectrum d_{ij} is written with the summation of each pure spectrum, a_{kj}, multiplied by its concentration, c_{ik} as follows:

$$d_{ij} = \sum c_{ik} a_{kj}. \tag{5}$$

Therefore, data matrix $\boldsymbol{D}$ can be decomposed as

$$\boldsymbol{D} = \boldsymbol{C}\boldsymbol{A}, \tag{6}$$

where $\boldsymbol{C}$ and $\boldsymbol{A}$ are respectively the matrices of the concentration profiles and the pure chemical component spectra. The rows and columns of $\boldsymbol{C}$ show the number of measured spectra (the number of samples) and the number of components, respectively. The rows and columns of $\boldsymbol{A}$ show the number of components and the number of data points for each spectrum. Our purpose is to obtain the physically meaningful $\boldsymbol{C}$ and $\boldsymbol{A}$, but it is generally impossible to determine $\boldsymbol{C}$ and $\boldsymbol{A}$ without additional information because the equation

$$\boldsymbol{D} = \boldsymbol{C}\boldsymbol{R}\boldsymbol{R}^{-1}\boldsymbol{A} = \boldsymbol{C}'\boldsymbol{A}' \tag{7}$$

has an infinite number of solutions for any arbitrary transformation matrix $\boldsymbol{R}$. There are two kinds of ambiguities in the matrix $\boldsymbol{R}$; one is the rotational ambiguity and the other is the intensity ambiguity. We used the constraint in which both concentrations and intensities of spectra are non-negative in order to remove the rotational ambiguity. All XANES spectra had been already normalized before applying the multivariate curve resolution method, so we removed the intensity ambiguity by normalizing each calculated spectrum with its edge jump at the end of calculation.

The initial matrix of $\boldsymbol{C}$, $\boldsymbol{C}_0$ was estimated by the use of the method called Evolving Factor Analysis (EFA),[16,17] and $\boldsymbol{C}_0$ was used for the

initial values in a constrained ALS calculation.[13,14] At each iteration of the calculation, new spectral profiles A and new concentration profiles C were obtained, as in the following two equations:

$$A = C^{+}\overline{D}, \tag{8}$$

$$C = \overline{D}A^{+}, \tag{9}$$

where C^{+} and A^{+} are the pseudoinverses of the matrices C and A.[15] They are expressed as $C^{+} = (C^{T}C)^{-1}C^{T}$ and $A^{+} = A^{T}(AA^{T})^{-1}$, where C^{T} and A^{T} are the transposes of the matrices C and A. The matrices C and A were calculated according to Eqs. 8 and 9. The negative elements of C and A are reset to zero at each iteration.

Results and Discussion

1. XANES Analyses. The Co K-edge XANES spectra before oxidation are shown in Fig. 1. The small pre-edge peak at 7.706 keV can be assigned to the 1s–3d transition and the intensity of the shoulder structure around 7.714 keV increases with the ratio Br/Co. Our previous work showed that such a spectral feature is related to the tetrahedral structure around Co.[18] This result, therefore, implies that the structure around Co has tetrahedral symmetry for large values of the ratio Br/Co. Since these spectra are the superposition of several kinds of Co complexes, this result indicates that the concentration of the tetrahedral complexes increases with Br/Co.

Figure 2 shows the XANES spectra after oxidation. The K-edge threshold energy shifts toward higher energy with the decrease of Br/Co. Since a lower energy position of Co K-edge in a Co complex is related to a lower oxidized state,[18] the complex with a larger ratio Br/Co is in a lower oxidized state. We consider that the complex with a larger Br/Co ratio is more difficult to be oxidized.

A series of spectral data before and after oxidation were sorted in matrix form, D_{before} and D_{after}, respectively. The number of dimensions of the matrices is 6 (the number of spectra) times 181 (the number of data points per spectrum). We also arranged the augmented column-wise matrix D_{all}, the number of whose dimensions is 12 (the number of spectra) times 181 (the number of data points per spectrum) by combining the data set before oxidation D_{before} and after oxidation D_{after}.

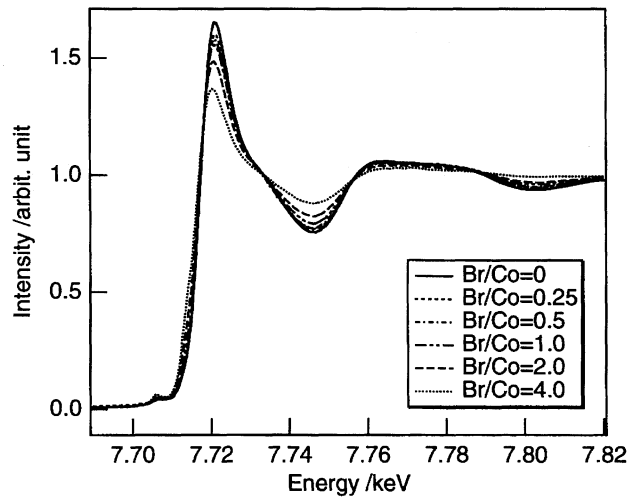

Fig. 1. The Co K-edge XANES spectra of the acetic acid solutions of the cobalt bromo complexes (before oxidation).

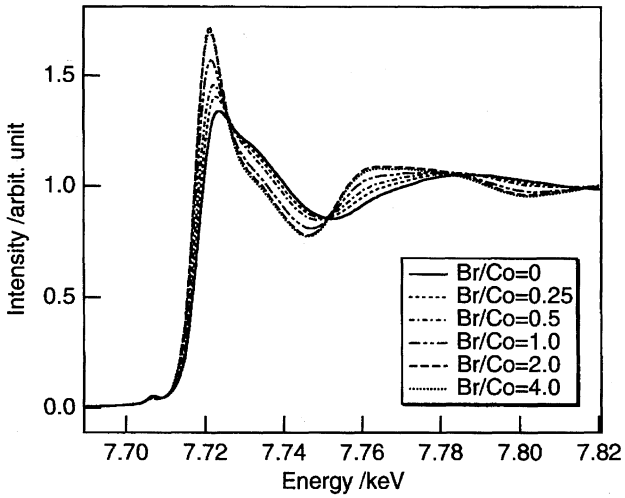

Fig. 2. The Co K-edge XANES spectra of the acetic acid solutions of the cobalt bromo complexes oxidized with ozone for two hours (after oxidation).

The plots of singular values are shown in Fig. 3. The two larger singular values seem to be significant in D_{before} (Fig. 3(a)) and D_{after} (Fig. 3(b)) compared with residual values which are very small. In the matrix D_{all} (Fig. 3(c)), the three values are considered to be significant. These results show that D_{before} and D_{after} both contain two pure components and that D_{all} contains three pure components. One of the components in D_{before} is therefore common to that in D_{after}.

Figure 4 shows the spectra extracted from the two different matrices D_{before} and D_{after} by the multivariate curve resolution calculation. The spectral shape of component 1 from D_{before} is exactly the same as that of component 1 from D_{after}, so we can say that the common component between D_{before} and D_{after} is component 1.

In Fig. 5, the extracted spectrum of component 1 is compared with the spectrum of $Co(CH_3COO)_2 \cdot 4H_2O$ which was measured as a standard divalent octahedral Co complex. It is clear that the spectrum of component 1 is almost the same as the XANES spectrum of $Co(CH_3COO)_2 \cdot 4H_2O$, so we conclude that component 1 is a complex with similar structure around Co to that of $Co(CH_3COO)_2 \cdot 4H_2O$, which should be the cobalt(II) acetate complex.

Figure 6 shows the comparison of the spectrum of component 2 in Fig. 4(a) with that of $K_2Co(SCN)_4$, which is a divalent tetrahedral Co complex. The spectral features of component 2 are not very similar to those of $K_2Co(SCN)_4$. Since the spectrum of $K_2Co(SCN)_4$, reported in our previous work,[18] was measured under different experimental conditions from this work, we can not compare it precisely and quantitatively with the spectrum of component 2. We find, however, that the pre-edge peak, which is assigned to the dipole-forbidden 1s–3d transition,[19] and the shoulder structure around 7.714 keV are common features in these two

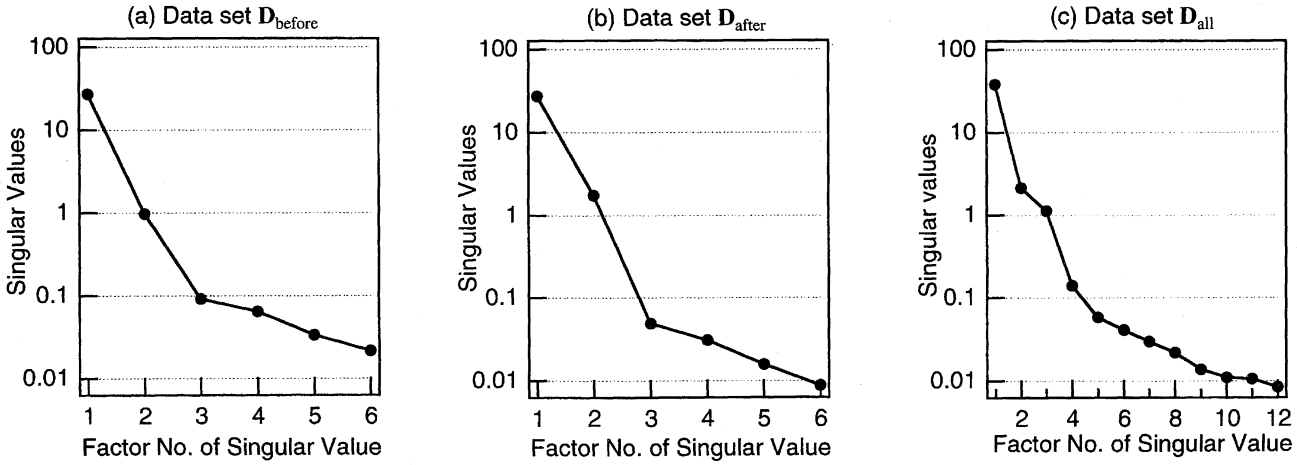

Fig. 3. The singular values of (a) data matrix $\boldsymbol{D}_{before}$, (b) data matrix $\boldsymbol{D}_{after}$, (c) data matrix $\boldsymbol{D}_{all}$. The singular values are plotted in order from the largest value to the smallest value decreasingly.

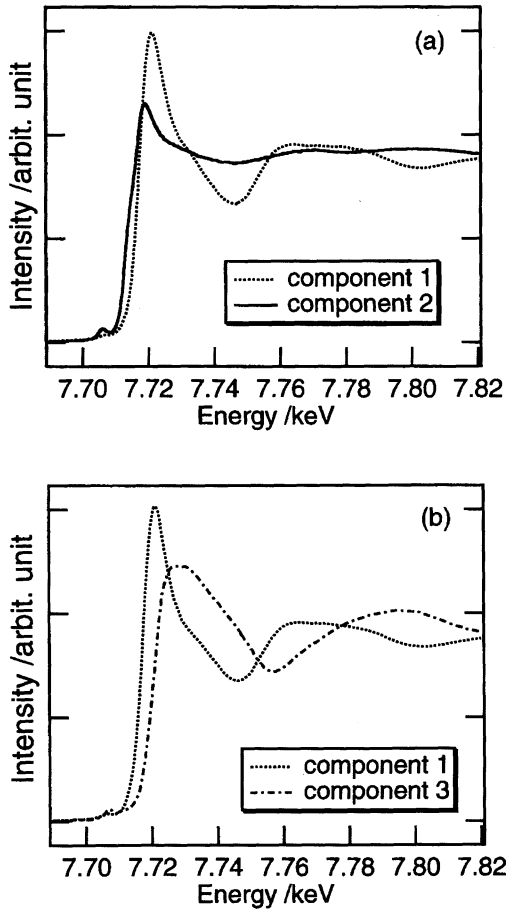

Fig. 4. The extracted Co K-edge XANES spectra from (a) data matrix $\boldsymbol{D}_{before}$, (b) data matrix $\boldsymbol{D}_{after}$.

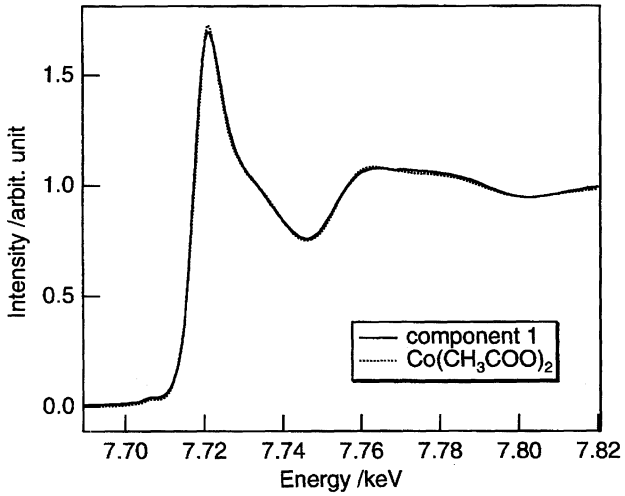

Fig. 5. The extracted XANES spectrum of component 1 and the measured Co K-edge XANES spectrum of Co-$(CH_3COO)_2 \cdot 4H_2O$.

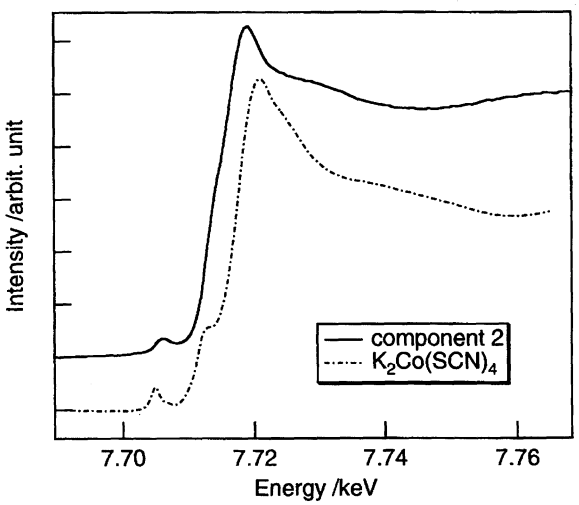

Fig. 6. The extracted XANES spectrum of component 2 and the measured Co K-edge XANES spectrum of $K_2Co(SCN)_4$ which was measured in previous work.[18]

spectra. It has also been reported that the intensity of the pre-edge peak of Mn compounds is stronger in tetrahedral symmetry than in octahedral symmetry.[20] This is considered to occur since the 3d orbitals of transition metal are partially mixed with the 2p orbitals of oxygen in tetrahedral symmetry. Therefore, component 2 is supposed to take the tetrahedral structure around Co.

The spectrum of component 3 shown in Fig. 4(b) is compared with those of $Co(acac)_3$ and $Co(CH_3COO)_2 \cdot 4H_2O$ in Fig. 7. The $Co(acac)_3$ XAFS spectrum was measured as a standard trivalent Co complex. The energy position of the K-edge is about 3 eV higher for component 3 than that for $Co(CH_3COO)_2 \cdot 4H_2O$, which is a divalent octahedral Co complex. The edge position and the pre-edge peak position are almost the same for component 3 and $Co(acac)_3$, which shows that component 3 is a trivalent complex of Co. The shape of the spectrum of component 3 is similar to that of $Co(acac)_3$ except for the energy region from 7.72 to 7.74 keV, which implies that component 3 has an octahedral structure around Co.

We conclude that the spectra before oxidation consist of two chemical species: One is the divalent octahedral Co complex having the same local structure as that of $Co(CH_3COO)_2 \cdot 4H_2O$ around Co and the other is the divalent tetrahedral Co complex. In the samples after oxidation, there are two chemical species: One is the divalent octahedral Co complex having the same local structure as that of $Co(CH_3COO)_2 \cdot 4H_2O$, and the other is the trivalent Co complex having the octahedral structure around Co.

The calculated relative concentrations of component 1, component 2, and component 3 obtained from $\boldsymbol{D}_{\text{before}}$ and $\boldsymbol{D}_{\text{after}}$ with multivariate curve resolution calculation are shown in Table 1. In these calculations, we assumed the total amount of the relative concentrations of the two components to be equal to 1.0 because the absolute concentration of Co does not change in each sample. The concentration of component 2 in the sample of the ratio Br/Co = 0.0 before oxidation is assumed to be zero because only cobalt(II) acetate is included in the sample. The concentration of component 2 increases with Br/Co in the samples before oxidation, which shows that component 2 is the complex coordinated by Br atoms. In the samples after oxidation, the concentration of component 3 decreases with increases of Br/Co. These results show that the oxidation of component 2 is more difficult than that of component 1. In other words, the results imply that the oxidation of the divalent tetrahedral Co complex coordinated by Br atoms is more difficult than that of octahedral of cobalt(II) acetate complex.

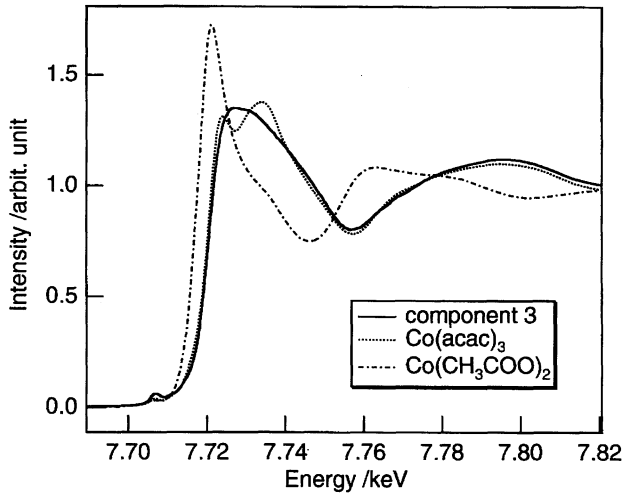

Fig. 7. The extracted XANES spectrum of component 3 and the measured Co K-edge XANES spectrum of $Co(CH_3COO)_2 \cdot 4H_2O$ and $Co(acac)_3$.

We think the reaction mechanism is as follows. At the first step, component 1 is oxidized with ozone and converted into component 3. Next, the Br ion in component 2 reduces component 3 to component 1 and at the same time the Br ion is oxidized by component 3 and removed from component 2. The oxidized Br does not have the capability of coordinating to Co complexes any more. As a result, the component 2 which reduces component 3 is changed into component 1 and is not reproduced. Component 2 is therefore not seen in the sample after oxidation in this oxidation condition. It is necessary to study the samples prepared in different conditions of the oxidation and measure Br K-edge XAFS spectra to elucidate the mechanism.

2. EXAFS Analyses. The Co K-edge EXAFS spectra $k^3\chi(k)$ of the data before and after oxidation are shown in Figs. 8 and 9. The phase and shape of EXAFS oscillation change clearly with Br/Co. Figures 10 and 11 show the results of their Fourier transforms. Before oxidation, the main peak around 1.6 Å shifts toward longer distances with increases of Br/Co. After oxidation, the largest peak shifts toward longer distances with increases of Br/Co, and the second largest peak observed at the ratio Br/Co = 0.0 becomes smaller with the increase of Br/Co.

In Tables 2 and 3, the structural parameters calculated from

Table 1. Concentrations of Component 1, Component 2, and Component 3 in Before and After Oxidation Using the Multivariate Curve Resolution Method

	Before oxidation		After oxidation	
Br/Co	Component 1	Component 2	Component 1	Component 3
0.0	1.00	0.00	0.44	0.55
0.25	0.95	0.05	0.55	0.45
0.5	0.89	0.11	0.65	0.35
1.0	0.83	0.17	0.83	0.17
2.0	0.66	0.34	0.97	0.03
4.0	0.40	0.60	0.98	0.02

In these calculations, we assumed that the total amount of the concentrations of two components is equal to 1.00 in each sample. The component 2 at Br/Co = 0 in the sample before oxidation is assumed to be zero.

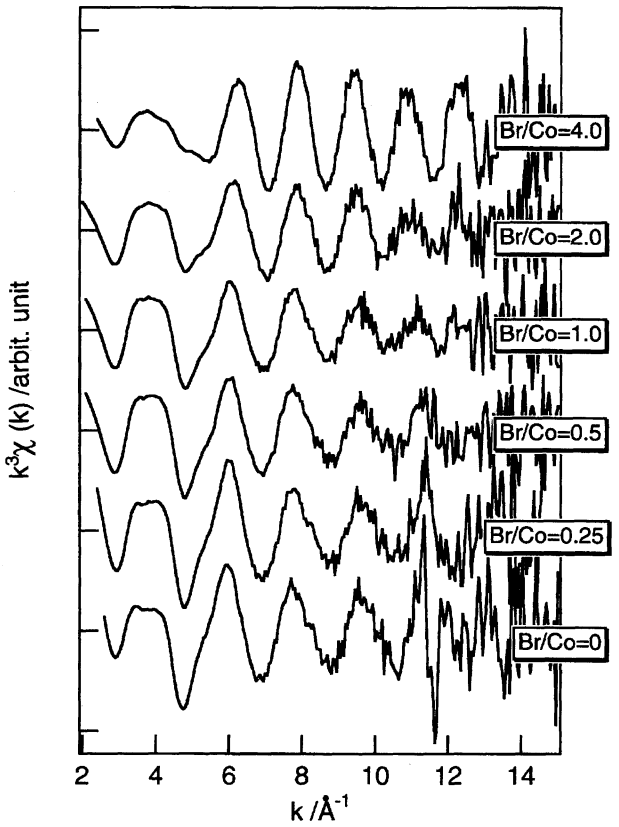

Fig. 8. The Co K-edge EXAFS spectra $k^3\chi(k)$ of the cobalt bromo complexes (before oxidation).

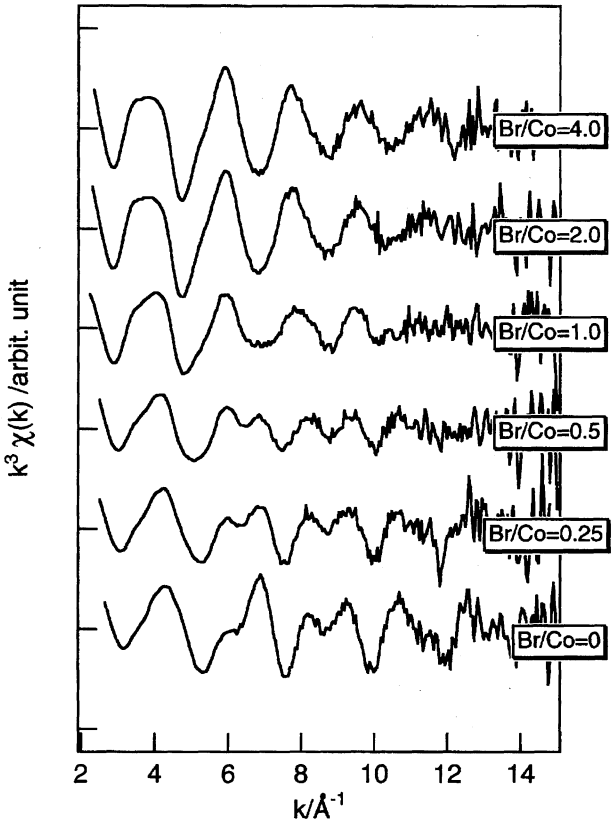

Fig. 9. The Co K-edge EXAFS spectra $k^3\chi(k)$ of the cobalt bromo complexes oxidized with ozone for two hours (after oxidation).

Table 2. The Inter-Atomic Distance (R) and Coordination Numbers (CN) from Curve Fitting Calculations in the Data Before Oxidation

	Co–O		Co–Br	
Br/Co	R (Å)	CN	R (Å)	CN
0.0	2.06	6.0	—	—
0.25	2.05	5.4	—	—
0.5	2.05	5.0	—	—
1.0	2.05	5.6	(2.40)	(0.7)
2.0	2.04	4.6	2.40	1.0
4.0	2.03	3.0	2.40	1.9

The values of Co–Br at Br/Co = 1 are not reliable because the contribution of Co–Br is quite small and the R factor is not good.

Table 3. The Inter-Atomic Distance (R) and Coordination Numbers (CN) from Curve Fitting Calculations of the Data After Oxidation

	$Co–O_1$		$Co–O_2$		Co–Co	
Br/Co	R (Å)	CN	R (Å)	CN	R (Å)	CN
0.0	*2.06*	1.5	1.85	2.4	2.86	1.2
0.25	*2.06*	1.8	1.85	1.9	2.86	0.9
0.5	*2.06*	3.0	1.86	1.6	2.84	0.6
1.0	*2.06*	4.4	(1.85)	(0.8)	(2.74)	(0.2)
2.0	*2.06*	6.1	—	—	—	—
4.0	*2.06*	6.1	—	—	—	—

The inter-atomic distances of $Co–O_1$ are kept fixed to 2.06 Å. The values of $Co–O_2$ and Co–Co at Br/Co = 1 are not reliable because the contribution of $Co–O_2$ ad Co–Co is small and the R factor is not good.

the curve fitting calculation are summarized. Two kinds of calculations were carried out, except in the case of the Br-free sample before oxidation. In the first calculation, one shell is assumed. In the second calculation, two shells before oxidation or three shells after oxidation are assumed. As the smaller R factor shows the better curve fitting result, we only show the best results in Tables 2 and 3. From the result of XANES, the samples after oxidation are considered to contain cobalt(II) acetate whose calculated inter-atomic distance Co–O is 2.06 Å in this work. We therefore fix the inter-atomic distance $Co–O_1$ equal to 2.06 Å in the calculation after oxidation in order to reduce the number of free parameters.

For the samples before oxidation with Br/Co ratios from 1.0 to 4.0, we detect Co–Br pairs whose Br coordination numbers increase with Br/Co. Since the concentration of component 2 increases with Br/Co as shown in Table 1 and in component 1 there is no Co–Br pair, we can say that the Co–Br pair exists only in component 2. The reason why we cannot find Co–Br pairs in the data of Br/Co = 0.25 and 0.5, is because the concentration of component 2 is too low. On the other hand, there exist Co–O pairs in both component 1 and component 2.

We estimated the coordination number of Br and O in

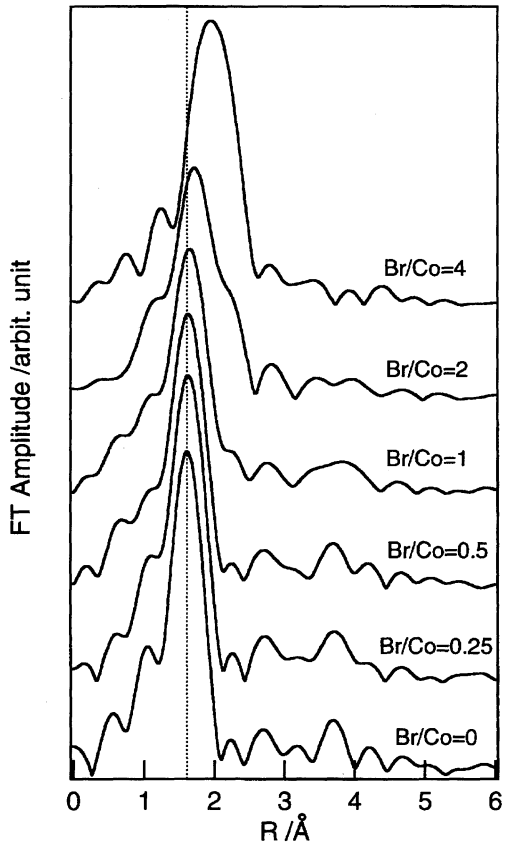

Fig. 10. The Fourier transforms of the EXAFS spectra $k^3\chi(k)$ of the cobalt bromo complexes (before oxidation).

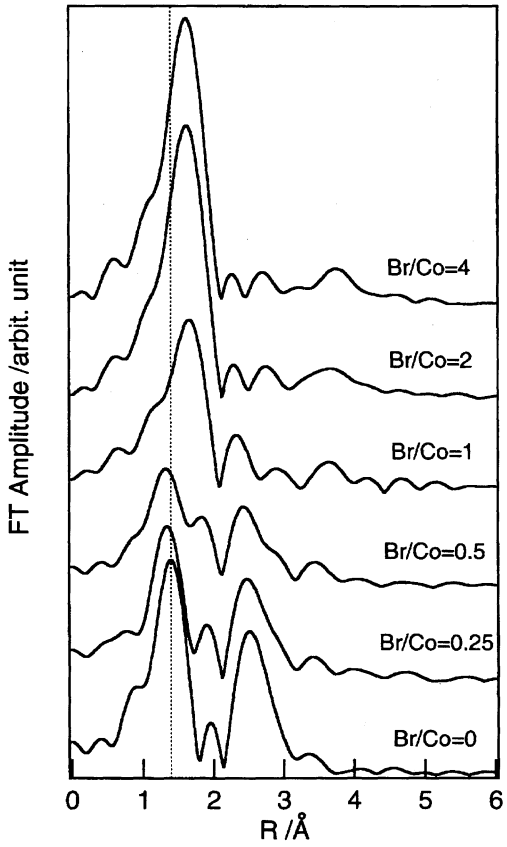

Fig. 11. The Fourier transforms of the EXAFS spectra $k^3\chi(k)$ of the cobalt bromo complexes oxidized with ozone for two hours (after oxidation).

component 2 by using the results at Br/Co = 2.0 and 4.0 shown in Tables 1 and 2. Since the Co atom in the cobalt(II) bromo complexes in acetic acid solutions is considered to be coordinated by the O atom of CH_3COOH, CH_3COO^- or H_2O and the Br atom in chemical equilibrium,[2] we assume that component 2 has a CoO_xBr_y cluster structure around Co. The results are shown in Table 4(a), which imply that component 2 has the Co complexes coordinated by one O and three Br ($CoOBr_3$), or by two O and two Br (CoO_2Br_2).

For the samples after oxidation with the ratio Br/Co from 0.0 to 1.0, Co–O_2 and Co–Co pairs are observed. The Co coordination number of a Co–Co pair decreases with the increase of the Br/Co. We cannot find any Co–Br pair in the Fourier transformed EXAFS results. We can therefore say that there exist Co–O and Co–Co pairs, but no Co–Br pair in component 3.

Table 4. The Estimated Coordination Number of Component 2 and Component 3

(a) Component 2 : CoO_xBr_y

Br/Co	x	y
2.0	1.9	2.9
4.0	1.0	3.2

(b) Component 3 : CoO_xCo_y

Br/Co	x	y
0.0	4.4	2.2
0.25	4.2	2.0
0.5	4.6	1.7

CoO_xBr_y in component 2 and CoO_xCo_y in component 3 are assumed in this estimations.

We estimated the coordination number of O and Co in component 3 by using the results for the ratios Br/Co from 0.0 to 1.0 shown in Tables 1 and 3. Since the trinuclear oxo-centered structure was reported in the oxidation of cobalt(II) acetate,[5] and Co–O and Co–Co pairs are found in component 3, we assume that component 3 has a CoO_xCo_y cluster structure around Co. The results are shown in Table 4(b), where the Co coordination number is two. The trinuclear oxo-centerd complex has three Co atoms which are triangularly connected with each other by CH_3COO^- and an O atom, where the Co–Co coordination number is two. Component 3 is therefore considered to be a Co trinuclear oxo-centered complex. It has been reported that the trinuclear oxo-centered complex was produced by the oxidation of cobalt(II) acetate in acetic acid solution with ozone.[5] On the other hand, the coordination number of O is about four. This is contrary to the result obtained from XANES analyses in this work and to the reported structure, which also has the six O atoms around Co. The Co–O_2 distance is not so different from the Co–O_1 distance, as shown in Fig. 11. The coordination numbers of Co–O_2 and Co–O_1 are therefore difficult to precisely estimate by the use of curve fitting. This is the reason why the calculated coordination number of O in component 3 is smaller than six, which is expected from the result of XANES and the reported structure. The EXAFS spectrum of each chemical species could also be extracted

with the multivariate curve resolution method, as was done in XANES analyses.

The results obtained here show that the complexes coordinated by Br atoms also change to trinuclear Co complexes without Br after the ozone oxidation, as observed for cobalt(II) acetate. The rate of the change from the Br-coordinated complex to the trinuclear Co complex is, however, smaller than that from the cobalt(II) acetate complex.

Conclusions

The present study clearly shows that the acetic acid solution of cobalt(II) bromo complexes for the ratio Br/Co from 0.25 to 4.0 have two different kinds of complexes in solution. One is the divalent complex $Co(CH_3COO)_2 \cdot 4H_2O$, and the other is the divalent tetrahedral complex; the central Co atoms are surrounded by two O atoms and two Br atoms, or one O atom and three Br atoms.

The oxidized sample with ozone consists of the divalent complex $Co(CH_3COO)_2 \cdot 4H_2O$ and the trivalent trinuclear complex with octahedral structure around Co, which would be the same complex as reported previously.[5] In this work, we have not found any complexes that include Br atoms after ozone oxidation.

The rate of the change from the Br coordinated complexes to the trinuclear Co complex is smaller than that from the cobalt(II) acetate complex. This indicates that the divalent tetrahedral cobalt(II) complex coordinated by Br is more difficult to be oxidized than the cobalt(II) acetate complex with the octahedral structure around Co. Further studies of the XAFS analyses in the transient region of the oxidation and Br K-edge XAFS spectra, are necessary to elucidate its mechanism.

We have successfully extracted each XANES spectrum from its overlapped spectrum by applying the multivariate curve resolution method. We find that the multivariate curve resolution method is very useful with multi-component systems. The multivariate curve resolution method will enable us to save time analyzing XAFS spectra because it is enough to analyze only the small number of pure spectra instead of each spectrum. Furthermore, since the spectra without the overlapping of spectra of other chemical components can be analyzed in XAFS analyses, we can get more reliable curve fitting results.

The authors would like to thank Professor Takashi Fujikawa of Chiba University for his useful comments, and would like to thank Professor Bruce Kowalski and Dr. David Veltkamp of the University of Washington for introducing the author to the multivariate curve resolution method. The multivariate curve resolution calculations were carried out in the Center for Process Analytical Chemistry (CPAC) at the University of Washington. This work has been performed through collaboration between Mitsubishi Chemical Corporation and the Institute of Materials Structure Science at the High Energy Accelerator Research Organization (KEK).

References

1) R. A. Sheldon and J. K. Kochi, "Metal-Catalyzed Oxidations of Organic Compounds," Academic Press, New York (1981).
2) K. Sawada and M. Tanaka, *J. Inorg. Nucl. Chem.*, **39**, 339 (1977).
3) M. Sano, T. Maruo, Y. Masuda, and H. Yamatera, *J. Solution Chem.*, **15**, 803 (1986).
4) D. P. Karim, P. J. Harget, and C. K. Saw, *Physica B*, **158**, 47 (1989).
5) A. B. Blake, J. R. Chipperfield, S. Lau, and D. E. Webster, *J. Chem. Soc., Dalton Trans.*, **1990**, 3719.
6) M. Nomura and A. Koyama, *KEK Rep.*, **95**, 15 (1996).
7) F. W. Lytle, R. Greegor, D. Sandstrom, E. Marques, J. Wong, C. Spiro, G. Huffman, and F. Huggins, *Nucl. Instrum. Meth.*, **226**, 542 (1984).
8) B.-K. Teo, "EXAFS Basic Principals and Data Analysis," Springer-Verlag, Berlin (1986).
9) J. J. Rehr, R. C. Albers, and S. I. Zabinsky, *Phys. Rev. Lett.*, **69**, 3397 (1992).
10) M. Fernándes-García, C. Márquez Alvarez, and G. L. Haller, *J. Phys. Chem.*, **99**, 12565 (1995).
11) S. R. Wasserman, *J. Phys. IV, Fr.*, **7**, C2-203 (1997).
12) E. R. Malinowski, "Factor Analysis in Chemistry," 2nd ed, John Wiley & Sons, New York (1991).
13) R. Tauler and B.Kowalski, *Anal. Chem.*, **65**, 2040 (1993).
14) R. Tauler, *Chem. Intell. Lab. Sys.*, **30**, 133 (1995).
15) H. Yanai and K. Takeuchi, "Projection Matrix, Generalized Inverse Matrix, Singular Value Decomposition," Tokyo-Daigaku-Shuppankai, Tokyo (1983) [in Japanese].
16) H. Gampp, M. Maeder, C. J. Meyer, and A. D. Zuberbühler, *Talanta*, **32**, 1133 (1985).
17) H. R. Keller and D. L. Massart, *Chem. Intell. Lab. Sys.*, **12**, 209 (1992).
18) T. Akai, M. Okuda, K. Horiuchi, J. Matsuura, Y. Koike, M. Yimagawa, and T. Fujikawa, *Jpn. J. Appl. Phys.*, **33**, 6360 (1994).
19) A. Bianconi, "EXAFS for Inorganic Systems," ed by C. D. Garner and S. S. Hasnain, Daresbury Laboratory. SERC DL/SCI/R17, (1981), p. 13.
20) M. Belli, A. Scafati, A. Bianconi, and E. Burattini, *Solid State Commun.*, **35**, 355 (1980).